Dossier

This paper is a part of the hereunder thematic dossier published in OGST Journal, Vol. 68, No. 2, pp. 187-396 and available online here

Cet article fait partie du dossier thématique ci-dessous publié dans la revue OGST, Vol. 68, n°2, pp. 187-396 et téléchargeable ici

DOSSIER Edited by/Sous la direction de : **Jean-Charles de Hemptinne**

InMoTher 2012: Industrial Use of Molecular Thermodynamics
InMoTher 2012 : Application industrielle de la thermodynamique moléculaire

Oil & Gas Science and Technology – Rev. IFP Energies nouvelles, Vol. 68 (2013), No. 2, pp. 187-396

IFP Energies nouvelles

Oil & Gas Science and Technology – Rev. IFP Energies nouvelles, Vol. 68 (2013), No. 2, pp. 309-318

DOI: 10.2516/ogst/2012047

Dossier

InMoTher 2012 - Industrial Use of Molecular Thermodynamics
InMoTher 2012 - Application industrielle de la thermodynamique moléculaire

Improving Molecular Simulation Models of Adsorption in Porous Materials: Interdependence between Domains

J. Puibasset

Centre de Recherche sur la Matière Divisée, CNRS Université d'Orléans, 1 bis rue de la Férollerie, 45071 Orléans Cedex 02 - France
e-mail: puibasset@cnrs-orleans.fr

Résumé — Amélioration des modèles d'adsorption dans les milieux poreux par simulation moléculaire : interdépendance entre les domaines — Le confinement de fluides est fréquent dans les systèmes naturels et industriels et se révèle très utile pour caractériser les matériaux poreux. L'outil essentiel de caractérisation consiste à mesurer les isothermes d'adsorption/désorption, c'est-à-dire la quantité de fluide adsorbée par le milieu poreux en fonction du potentiel chimique (ou de la pression relative). Les modèles utilisés pour analyser les données sont en général très simples, conduisant à des caractérisations imprécises des matériaux. En particulier, la non prise en compte de l'interdépendance entre les pores élémentaires (ou domaines) entraine des conclusions erronées. Notre approche propose de résoudre ce problème dans le cadre d'une approche par simulation moléculaire.

Abstract* — *Improving Molecular Simulation Models of Adsorption in Porous Materials: Interdependence between Domains — *Fluid confinement is ubiquitous in nature and industry, and is the most widely used technique to characterize porous materials. The main characterization tool consists in measuring the so-called adsorption/desorption isotherms,* i.e. *the amount of gas adsorbed by the porous substrate as a function of the fluid chemical potential (or relative pressure). The models used to analyse the data are generally quite simple, leading to inaccurate characterization of the porous materials. In particular, ignoring the interdependence between the elemental pores or domains leads to inappropriate conclusions. Our approach proposes to cure this problem in the molecular simulation approaches.*

INTRODUCTION

Adsorption of fluids in porous materials has been known for more than one century. It is frequently encountered in nature and has many applications in industry. The most well-known natural examples are water or petroleum confined in porous rocks. Among the industrial examples, one can cite catalysis, gas storage, etc. [1, 2].

Two very different situations involve adsorption. In the first case, one is interested by the fluid. The porous material can be seen as a reservoir, which contains but also interacts with the fluid. These interactions have a non-negligible effect on the properties of the confined fluid. On the other hand, one may be interested in the porous material and use the fluid adsorption and the associated modifications of fluid properties to have access to some information regarding the porous material geometry [3, 4].

One of the first links established between pore geometry and adsorbed fluid property is through the macroscopic Kelvin equation [5]. More than one century ago, it has been observed that condensable gases may be in a dense (liquid-like) state even below the saturating pressure when confined in porous materials like charcoal. This phenomenon, the capillary condensation, may be seen as a shift of the liquid/vapor coexistence to lower pressure. The above mentioned Kelvin

equation gives a quantitative relation between the pore radius and this shift in vapor pressure (or liquid/vapor coexistence). Note that, more accurately, it is actually the curvature of the interface between the adsorbed liquid and the gas which appears in the equation. It is closely related to the pore geometry as long as the liquidlike layer of adsorbed fluid is thin (which is the case in the first stage of adsorption).

Of course, interfacial phenomena are involved in adsorption. The Kelvin equation mentions the surface tension of the liquid/vapor interface, as a result of a combined contribution of solid/vapor and solid/liquid interfacial energies, where the solid denotes the porous material walls. As a general trend, the smaller the pores, the larger the contribution of interfaces to the free energy, compared to bulk contributions. This is why adsorption phenomena are enhanced in nanoporous substrates (zeolites, charcoal, clays, etc.).

Since the very early work by Zigmondy [5], many improvements have been achieved in understanding the effects of confinement on fluid properties, in particular thermodynamic properties. Beside the shift in liquid/vapor coexistence, one of the most striking effects is the appearance of a hysteresis. After saturation of the porous material upon adsorption of a condensable gas, desorption does not superimpose on the adsorption curve. The adsorption curve is obtained by controlling the temperature of the system and by progressively introducing gas, which results in an increase in the pressure of the vapor above the material. The so-called adsorption isotherm measures the amount of fluid adsorbed in the material as a function of the chemical potential of the adsorbate given by the gas pressure above the substrate. The desorption curve is obtained during the release of the gas in the reservoir. This adsorption/desorption hysteresis has been interpreted by Cohan *et al*. [6] as a consequence of the dissymmetric shape of the liquid/vapor interface upon adsorption and desorption. Upon adsorption the gas adsorbs on the walls and thus the liquid/vapor interface follows the local geometry of the pore. On the other hand, desorption is thought to proceed in a different way. At saturation, the pores are entirely filled by liquidlike fluid, and liquid/vapor interfaces are rejected to the porous material boundaries. Upon desorption, these liquid/vapor menisci recede within the porous material, until gas has entirely replaced the liquid. In such a situation, the liquid/vapor interfaces are now hemi-spherical (if the contact angle is null) instead of following the shape of the pore. Figure 1 gives a scheme for a cylindrical pore. As can be seen, the curvature significantly differs in the two situations (factor 2), which results in very different values for the chemical potentials characterizing the capillary condensation (steep rise in adsorption) and capillary emptying (steep decrease during desorption). These interpretations are however inaccurate in real pores, as has been shown by Coasne *et al*. [7]; Grosman and Ortega [8].

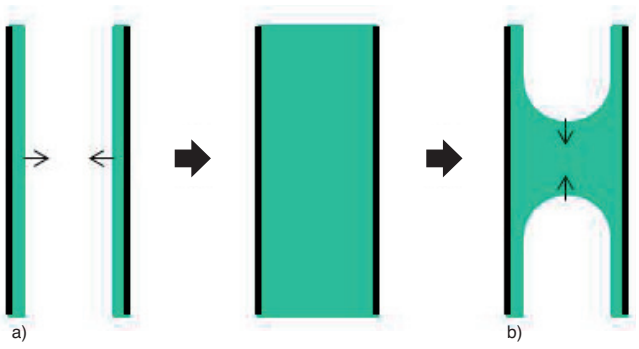

Figure 1

Schematic representation of the liquid/gas interface upon a) adsorption and b) desorption.

Interfaces appear to be the key parameter to understand adsorption. In nanoporous materials, interfacial contributions to the free energy are dominant. Many efforts have thus been devoted to the interpretation of adsorption experiments by means of interfacial theories. They lead to an accurate description of fluid structure and dynamics when adsorbed on a surface. The simplest situations (simple fluid adsorbed on crystals) can be treated in the framework of *ab initio* approaches, leading to accurate description of adsorbed fluid without any adjustable parameter. More complicated situations require larger-scale methods. This is the case if one considers fluid adsorbed on disordered (amorphous) substrate, which may present atomistic roughness and/or a local curvature at nanometric scale. Figure 2 proposes an overview of the various scales relevant to adsorption and the associated theoretical approaches. From this point of view, molecular simulation appears as a perfect tool able to take into account the physico-chemical characteristics of the porous materials at nanometric scale, as long as one has access to this information.

1 IMPROVING MODELISATION OF FLUID ADSORPTION

Molecular simulation of realistic situations reveals several difficulties. For instance, due to computational limitations, pores larger than 10 nm are difficult to handle. It is however in principle feasible to interpolate between the molecular simulation results in small pores (< 10 nm) and classical thermodynamic approaches in large pores (> 50 nm) where the Kelvin equation is expected to lead to correct results. But such interpolations may be erroneous for complicated pore geometries, or when long range interactions are involved. Furthermore, the complex structure of the porous network cannot be treated in a molecular simulation approach. As introduced by Everett and Whitton [9]; Everett and Smith [10]; Everett [11], a porous material can be seen as a collection of domains corresponding to elemental subdivision of the porous network. For instance, in a zeolite, the domains would correspond to elemental cavities. The most frequently

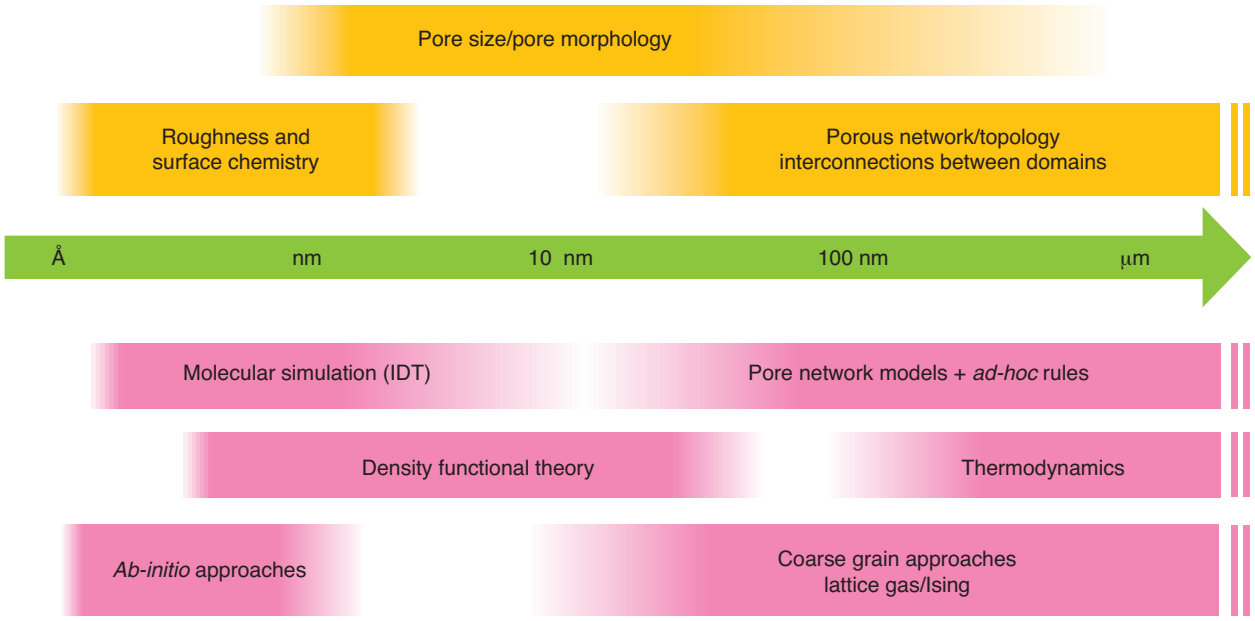

Figure 2

Above: Overview of the various scales relevant to porous materials; below: examples of theoretical models or approaches.

used approach consists in considering that the domains are independent. The global thermodynamic properties are thus obtained as an average over the domain distribution. When typical domains are of nanometric scale, molecular simulation is able to treat each of them independently and thus provides a powerful analysis of fluid adsorption after averaging over the appropriate distribution of domains. This approach leads to an extremely accurate description of the low pressure region of the adsorption isotherm, where the hypothesis of independence between domains is well satisfied.

But the hysteresis region is not well described by this approach. The porous network (and the associated large-scale disorder) plays an important role. This has been anticipated a long time ago, thanks to (simple) network models. Mason [12, 13] developed an original approach where the hysteresis shape is related to the nature of the interconnected network or pores. Swift *et al*. [14] have also studied the combined effect of confinement and interconnectivity in Ising-like models. Very recently, Kierlik *et al*. [15, 16] introduced a coarse grained approach which allowed to interpret the hysteresis loop as the signature of a very irregular energy landscape with many local minima induced by the disordered porous substrate. Such models also allow to study the large-scale structure of the confined fluid and the distribution of associated metastable states [17, 18]. What do we learn with these models? The fluid adsorbed in a given domain is obviously influenced by what can be found in the neighboring domains. There are however two different situations. In some cases, the fluid state in any given domain is uniquely defined as long as the temperature and chemical potential (and any other thermodynamic parameter) are given. In other cases, the fluid state in a given domain may not be uniquely defined even for imposed thermodynamic parameter. This may occur for instance if more than one metastable state is possible. If the barrier between the two states is significantly larger than thermal fluctuations, the system may remain trapped in one of the metastable states. For instance, a fluid adsorbed in an ink-bottlelike pore may, for some chemical potential values, either be adsorbed at the walls or fill the cavity. The metastable state will generally depend on system history, and, most importantly, may also depend on the fluid state in the neighboring domains. In this case, the porous network plays a fundamental role. The above mentioned network models deal with such situations, with various level of accuracy in the characterization of the metastable states. Extremely simplified models reduce to “empty/filled” two-state domains (bi-stable domains, Ising models, etc.) but more sophisticated models have been considered, which include more realistic features like the adsorbed film for instance. These features are generally deduced from a classical thermodynamic analysis of fluid adsorption in pores. However, significant improvement can be achieved if one uses molecular simulation to extract the rules allowing to determine the possible metastable states.

Molecular simulation thus appears as powerful tool to study fluid adsorption in elemental nanoscale cavities or domains, since the relevant fluid/fluid and fluid/substrate interactions are described at molecular level. However, due to computer limitations, it is not possible to take directly into account the complex network of interconnections between the various domains or heterogeneities which span up to micrometer scale. As a consequence, molecular simulation generally provides a good description of fluid adsorption at low coverage where the domains are approximately independent, but it is inefficient in the hysteresis region because molecular simulation is unable to take into account the large scale spatial distribution of heterogeneities in the pore network which have proven to play an important role in the hysteresis region. In this work, a multiscale approach is introduced, allowing both a molecular description of fluid/fluid and fluid/substrate interactions, and simultaneously taking into account the connectivity between the various domains constituting the porous material.

2 MOLECULAR MODEL AND METHODS

In order to show the importance of interdependence between domains, this study will focus on simple fluid adsorption in the frequently encountered silica-based nanoporous materials like MCM-41 or oxidized porous silica. These materials exhibit parallel and non-interconnected tubular pores with a high aspect ratio (few nanometers in diameter and few microns of length) [19-21]. Besides the atomistic disorder which is naturally taken into account in a molecular simulation approach, one should take care of the possible physico-chemical variations at nanometer scale along the pore axis [22-26]. Such variations most probably arise during the fabrication of the material, and could in principle be obtained by numerical reconstructions. These variations result in a modulation of the affinity of the adsorbed fluid (argon in our case) with the wall. We have in particular shown that pore size variations actually predominantly result in variations of fluid/wall interactions, with moderate "purely geometric" effects [27-30]. As a simplification, the corresponding heterogeneities are characterized by a single parameter which varies along pore and measures the intensity of the fluid/wall interaction. More precisely, this parameter is an extra factor applied to the fluid/wall interaction. Values less than 1 (down to 0.7 in our model) represent domains with lower affinity for the fluid. Values larger than 1 (up to 1.3 in our model) represent domains with higher affinity for the fluid.

The mesopore (3 nm in diameter) is drilled in an initial substrate made of pure silica of density close to the expected one (mesoporous silica walls are expected to be made of amorphous silica). Figure 3 gives a picture of the result. The fluid/fluid and fluid/substrate interactions are modeled by the (6-12) Lennard-Jones intermolecular potential cut and shifted at 2.5 σ, which is accurate enough to catch the main features of simple fluid adsorption. The parameters for argon are $\sigma_{Ar\text{-}Ar}$ = 0.3405 nm and $\varepsilon_{Ar\text{-}Ar}/k$ = 120 K where k is Boltzmann constant, and the parameters for argon/silica interactions are $\varepsilon^0_{Ar\text{-}O}/k$ = 100 K and $\sigma_{Ar\text{-}O}$ = 0.333 nm (fluid/wall interactions are mainly with O species).

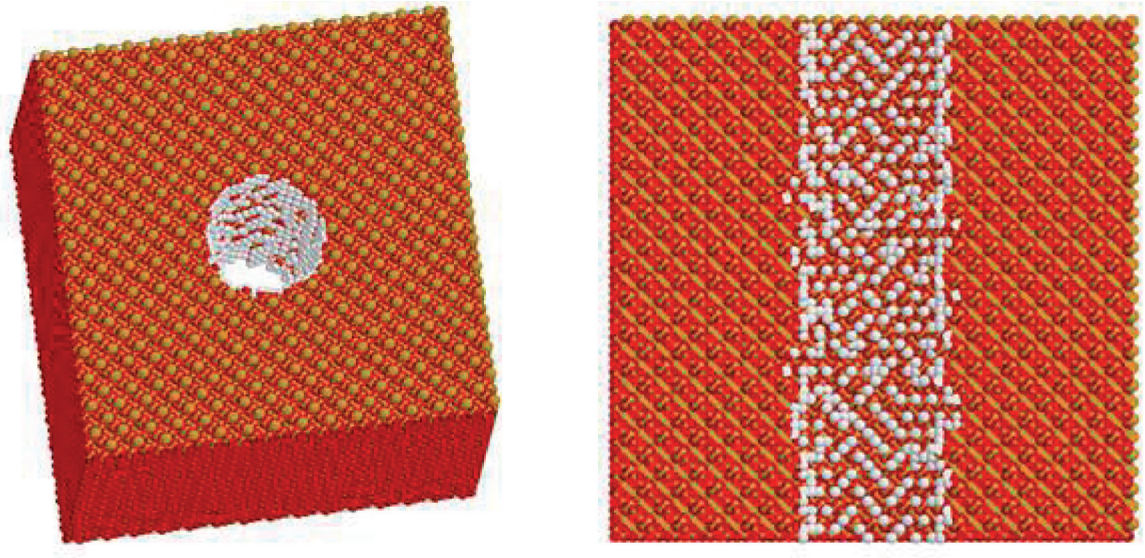

Figure 3

Molecular configuration showing the 3 nm pore drilled in a pure silica substrate (cristobalite). The dangling bonds produced by the drilling are replaced by surface hydroxyls. Yellow: silicon. Red: oxygen. White: Hydrogen. The atomic roughness is visible on side view.

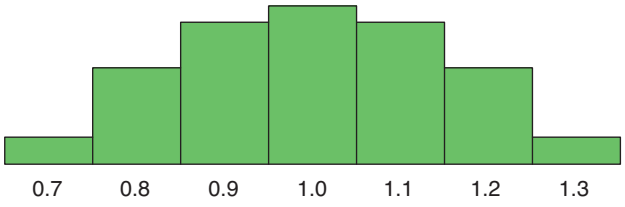

Figure 4

Discrete Gaussian distribution of heterogeneities (associated to domains) introduced in the micrometric pore.

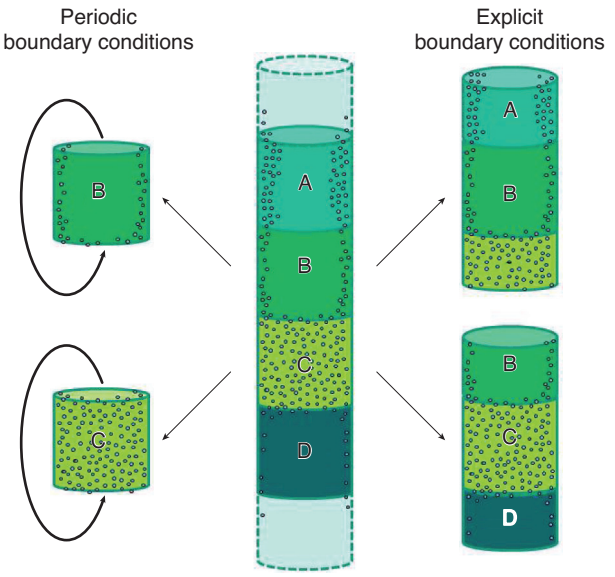

Figure 5

Schematic representation of two methods to treat the heterogeneous pore shown in the middle. Left: all domains are treated separately, with the usual periodic boundary conditions (hypothesis of independent domains). Right: all domains are treated while keeping information regarding their local environment (two neighbors in this 1 dimensional case), by introducing explicit boundary conditions.

The physico-chemical heterogeneities in the porous substrate are approximated by a modulation over the porous substrate of the fluid/wall interaction intensity $\varepsilon_{Ar\text{-}O}$ around its typical value $\varepsilon^0_{Ar\text{-}O}$, within ±30%. This modulation typically defines domain size of few nanometers and we have arbitrarily chosen the value 7.36 nm for the simulations. It is emphasized that choosing 5 nm or 15 nm would not change the results obtained in this work. A typical pore then contains several hundreds of domains. The heterogeneity parameter $h = \varepsilon_{Ar\text{-}O}/\varepsilon^0_{Ar\text{-}O}$ is supposed to be constant within each domain and to take uncorrelated values between two adjacent domains. Its value within a given pore is supposed to follow a Gaussian distribution (see *Fig. 4*).

The simulations are performed using the grand canonical Monte Carlo algorithm [31, 32]. The chemical potential of argon is imposed and related to the gas pressure in the reservoir using the ideal gas relation since it is a good approximation at the temperature at which the simulations are performed ($T^* = Tk/\varepsilon_{Ar\text{-}Ar} = 0.6$, which corresponds approximately to 70 K). All adsorption/desorption results are given as a function of the reduced chemical potential $\mu^* = \mu/\varepsilon_{Ar\text{-}Ar}$. Long simulations are performed in order to reduce the uncertainties down to 7%, taking into account the correlation between successive configurations (10^8 Monte Carlo trials per argon where required).

How do we take into account the interdependence between the domains? In usual molecular simulations, each domain is treated independently, and periodic boundary conditions are used to minimize trivial spurious effects due to open boundaries (see *Fig. 5*). In this work, the periodic boundary conditions are modified to take into account the fluid state in the neighboring domains (see *Fig. 5*). Since interactions and correlations are short ranged, the nearest neighboring domains alone need to be considered. In other words, the fluid behavior in a given domain is not directly influenced by the fluid state in distant domains. Further simplifications may actually be made. Due to the very short range of the interactions in our model (2.5 σ), only the portion of the neighboring domains defined by this range need to be considered for the calculations. As a matter of fact, the fluid beyond this range has no direct influence on the fluid adsorbed in the central domain. Furthermore, these neighboring domains may be taken as homogeneous cylindrical pores with the physico-chemical characteristics of the studied domain (same pore size and fluid/wall interactions for instance). This is because the main effect of the neighboring domains does not originate in their detailed physico-chemical properties. The relevant information is the absence or presence of fluid in the neighboring domains and the corresponding density. The simulation box then contains the central domain (length: 7.36 nm = 21.6 $\sigma_{Ar\text{-}Ar}$) and two adjacent domains (taken to be 3 $\sigma_{Ar\text{-}Ar}$ long, see *Fig. 6*) which play the role of boundaries, where the fluid state (gaslike or liquidlike) is imposed during the calculations. Note that the molecular configurations of argon confined in these boundaries are not fixed: they are generated during the course of the simulation. As a consequence, these segments need their own boundaries. Here again, the details of the fluid state close to these boundaries are actually not relevant: the important point being to impose the fluid state (gaslike or liquidlike). We then just need to define an additional region (2 $\sigma_{Ar\text{-}Ar}$ long) at both pore ends (see *Fig. 6*) where an extra contribution is added to the external potential to maintain the fluid in the desired state: an extra attractive potential $-5\,\varepsilon_{Ar\text{-}Ar}$ allows to impose the liquidlike state, and an extra positive potential $+5\,\varepsilon_{Ar\text{-}Ar}$ allows to impose the gaslike state.

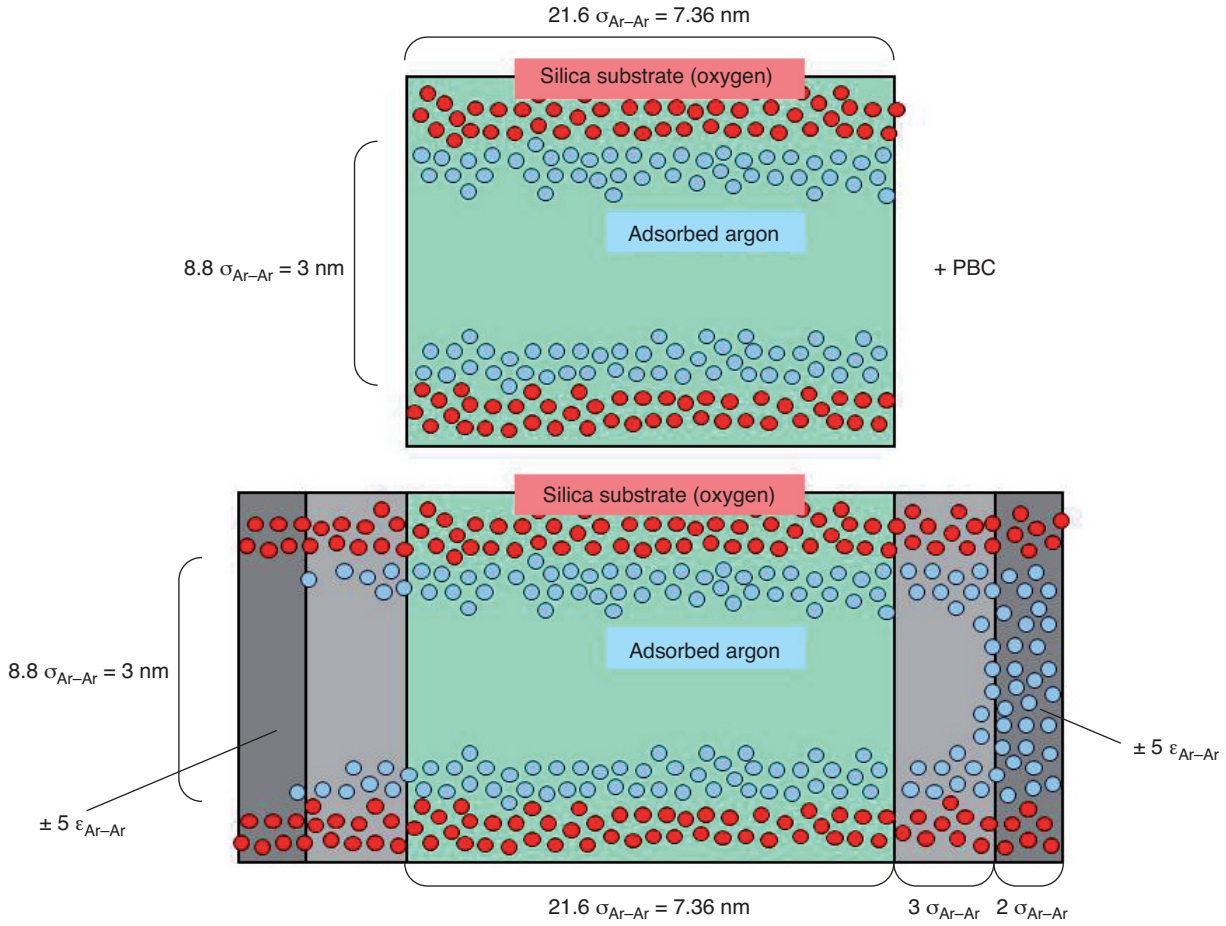

Figure 6

Schematic representation of the simulation box, showing the dimensions, the oxygen atoms from the silica substrate (red) and the adsorbed Argon (blue). Upper panel: With usual periodic boundary conditions, when a molecule gets out of the box on one side, it re-enter the box on the opposite side; lower panel: with explicit boundary conditions, when molecules in the domain under study (in green) approach the boundaries, they interact with molecules in the grey region which mimic the neighboring domains.

Simulation results (given in *Fig. 7, 8*) show that each domain behaves essentially as a bi-stable system. For independent domains (treated with periodic boundary conditions, *Fig. 7*), the adsorption/desorption isotherm exhibit a large hysteresis. The fluid may either follow the gaslike branch, denoted *G*, corresponding to the fluid adsorbed only at the walls, or follow the liquidlike branch, denoted *L*, corresponding to the fluid filling the whole domain. The transition between both is determined by the stability limits of both branches (corresponding to the nucleation of the first drop, or the first bubble). Note that a single loop is obtained. In the case of interdependent domains *(Fig. 8)*, several cases depending on the neighboring state have to be considered, producing three "conditional isotherms". The fluid may still either follow the gaslike or the liquidlike branches. However, the condensation occurs either at equilibrium (μ_{eq}) if one neighbor is liquidlike or is delayed (μ_{GG} corresponds to liquid nucleation). The domain emptying occurs at μ_{eq} if one neighbor is gaslike or is delayed (μ_{LL} corresponds to cavitation). Calculations show that these conditional isotherms depend on the modulation factor in the considered domain but are independent of it in the neighboring domains. This greatly simplifies the problem.

The conditional isotherms are calculated for all values of the modulation factor. Once these conditional isotherms are known, simple algorithms may be used to determine the fluid behavior in any given pore sample (adsorption/desorption isotherms, scanning curves, metastable states). Any change in μ impacts continuously on the fluid adsorbed in all domains and possibly induces transitions in few domains. This affects the fluid status in the neighboring domains and may trigger subsequent transitions (avalanche), until a new metastable state is reached.

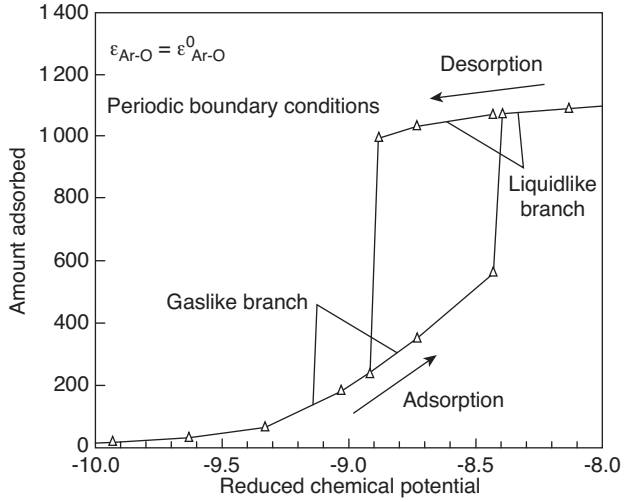

Figure 7

Typical adsorption/desorption isotherm obtained in a single domain with periodic boundary conditions. Triangle: Grand canonical Monte Carlo results. Lines are guide to the eye.

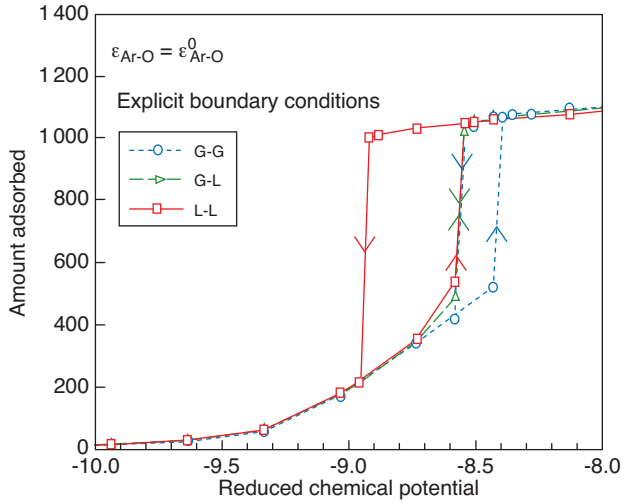

Figure 8

Typical conditional adsorption/desorption isotherms obtained in a single domain with explicit boundary conditions. Symbols: Grand canonical Monte Carlo results. Lines are guide to the eye. Blue/circles: G-G boundaries. Green/triangles: G-L boundaries. Red/squares: L-L boundaries.

3 ANALYSIS OF FLUID ADSORPTION/DESORPTION ISOTHERMS

The results for fluid adsorption/desorption isotherms are shown in Figure 9. For comparison, the results obtained with the interdependent domains and those within the usual hypothesis of independence of domains are superimposed. As can be seen, both isotherms are identical outside the hysteresis, but differ significantly in the hysteresis region. This confirms that the

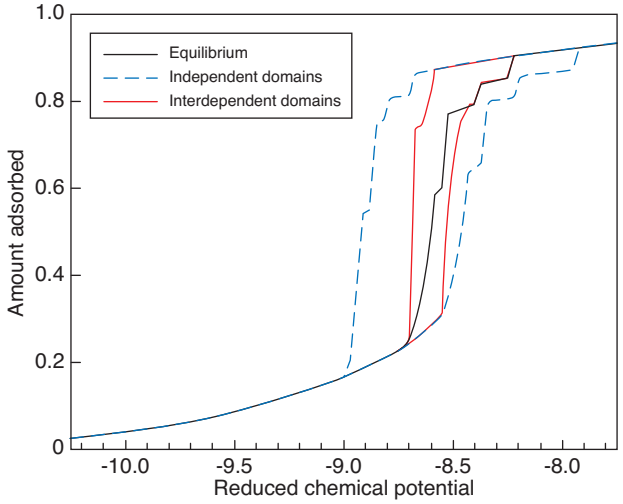

Figure 9

Adsorption/desorption isotherms for the entire pore (1 μm long, 140 domains) obtained with the two hypothesis: blue/dotted lines: independent domains; red/thick lines: interdependent domains; black/thin line: equilibrium.

hypothesis of independence between domains is acceptable when the fluid state is uniquely defined in each domain, while the interdependence has to be taken into account in the hysteresis region where some domains (but not necessarily all of them) have several metastable states. The main result is that taking into account the interdependence produces a significantly smaller hysteresis. The data also show that the adsorption branch is smoothly increasing due to the presence of the heterogeneities, while the desorption branch is almost vertical (triangular shape of the hysteresis). This suggests that collective effects occur upon desorption (to be re-discussed later). Another important difference between both cases is that the equilibrium curve meets the steep adsorption branch before the highest closure point, and meets the rapid desorption curve at the lowest closure point. This means that, in our model, adsorption does not occur at equilibrium, even just above the lowest closure point, and desorption does not occur at equilibrium even just below the highest closure point. This questions the frequently admitted hypothesis that desorption occurs at equilibrium and can thus be used to evaluate the pore size distribution. Actually, none of the branches is at equilibrium, and hence the standard methods to obtain pore size distributions are poorly justified. It is however shown by Figure 9 that, in our model, the adsorption branch meets the equilibrium curve before the higher closure point.

The above mentioned triangular shape of the hysteresis is closely related to the adsorption/desorption mechanism induced by the interdependence between domains. This mechanism can easily be extracted from the simulations. The results are given in Figures 10 and 11. As can be seen, the

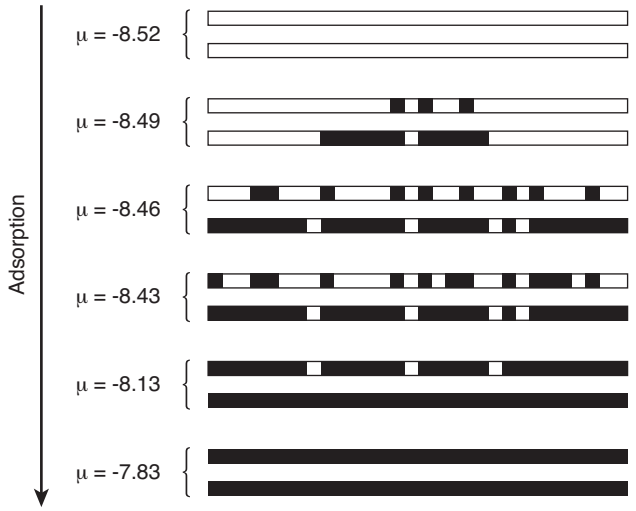

Figure 10

Schematic representation of the fluid state in a portion of the pore comprising 30 domains. Each square represent a domain. White: gaslike (fluid adsorbed at the wall). Black: liquidlike (dense fluid filling the domain). From top to bottom: increasing chemical potential (adsorption). For each chemical potential, the upper string is obtained within the hypothesis of independent domains, while the lower string is for interdependent domains.

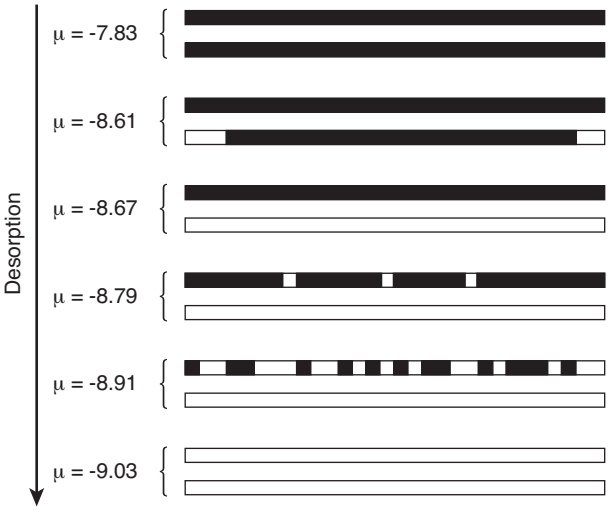

Figure 11

Same as Figure 10 for desorption (decreasing chemical potential from top to bottom).

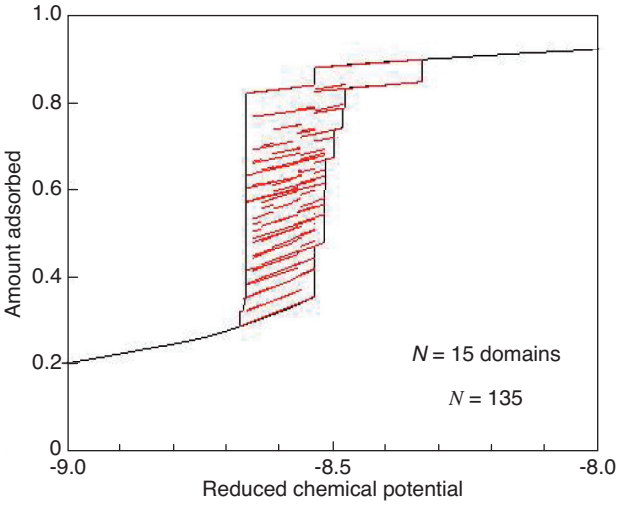

Figure 12

Example of all metastable states (135 in this case) which can be found for a small pore comprising only 15 domains with various fluid/wall affinities. Each metastable state has a lower and an upper stability limit, represented by a finite portion of (red) line. The lowest (highest) metastable state has semi-infinite extension and correspond to the beginning (end) of the gaslike (liquidlike) branch.

mechanism of adsorption and desorption are drastically affected by the hypothesis of independence between domains. In this case, adsorption proceeds "randomly" in the pore, starting with the most attractive domains (which are randomly distributed in the pore) and subsequently filling the remaining domains with the highest affinity. When taking into account the interdependence between domains, the very first stage of adsorption is still random (it occurs on the most attractive domains) but then adsorption proceeds *via* growing of these initial seeds (which play the role of nucleation centers). A similar behavior is observed upon desorption: within the hypothesis of independent domains, evaporation occurs randomly within the pore, according to the domains affinity, while taking into account the interdependence between domains induces a rapid emptying of the pore by recession of the liquid/gas menisci from the pore ends.

An important feature regarding hysteresis is the existence of metastable states inside the loop, which is a direct consequence of the possibility to perform adsorption/desorption scanning curves inside the loop [3, 4, 33]. Most of simulation works produce "empty" hysteresis, *i.e.* without any metastable state inside. See for instance reference [34] for a review on theoretical and simulation investigations and comparison with experiments. This fact is expected in simple pore geometries but it is also observed in more realistic disordered porous materials [35-38]. In order to produce metastable states inside the hysteresis, one has to introduce physico-chemical heterogeneities [39]. In the hypothesis of independent domains, these metastable states correspond to the juxtaposition of gaslike or liquidlike domains. Simple combination analysis leads to macroscopic results: the metastable states are always inside the main adsorption/desorption loop. Their number grows exponentially with system size, more specifically as 2^N

where N is the number of domains. The number 2 comes from the fact that each domain behaves like a bi-stable system. One generally introduces the complexity to characterize this exponential growth, as the normalized logarithm of the number of metastable states [40-43]. This complexity is ln2 (≈ 0.69) for independent bi-stable domains. What do we learn when taking into account the interdependence between domains? An example is given in Figure 12. Systematic exploration with various system sizes shows that all metastable states are always inside the hysteresis loop. The main adsorption/desorption loop is actually the envelope of the metastable states. Furthermore, the number of metastable states which can be found in the pore is significantly (exponentially) reduced. Their number still grows exponentially with system size, but the associated complexity is now 0.23, much less than ln2. This results from the fact that the interdependence between domains kills almost all "naïve" metastable states obtained as a combination of the two possible states for each domain. It is emphasized that heterogeneities favor metastable states, while interdependence between the various domains destabilize most of the metastable states.

CONCLUSION

Fluid adsorption in porous silica has been studied by molecular simulation. The porous material is seen as a collection of domains, with more or less affinity for the adsorbent (argon in our case). These heterogeneities are introduced in order to take into account the experimental observations of surface corrugation in silica pores at various length scales. Similar studies always neglect the interdependence between domains. In this work, we introduce a multi-scale approach which allows to perform the atomistic simulations while taking into account the effect of neighboring domains. To do so, the usual periodic boundary conditions usually applied to each domain are replaced by appropriate explicit boundaries. The results show drastic effects of interdependence between domains on adsorption/desorption isotherms, the mechanism of adsorption/desorption and existence of metastable states inside the loop. The adsorption or desorption proceed only *via* nucleation into the various domains if they are independent, while nucleation + menisci propagation is at work when the interdependence between domains is taken into account. This has drastic consequences on the main adsorption desorption isotherms: the hysteresis is much narrower when domains interact. We also observe that the number of possible metastable states is actually significantly reduced compare to the naïve picture of independent domains. Further studies will focus on a more realistic description of the heterogeneities, closer to experimental observations. It is hoped that such approach will allow a better analysis of adsorption experiments performed for porous materials characterization.

ACKNOWLEDGMENTS

Dr. A. Grosman, Dr. A. Delville, Dr. E. Kierlik, Dr. P. Porion and Dr. G. Tarjus are gratefully acknowledged for fruitful discussions on adsorption in porous materials. The simulations were performed on workstations purchased thanks to grants from *Région Centre* (France) and on IBM SP4 supercomputers at the *Centre de Ressources Informatique de Haute Normandie* (CRIHAN, St-Etienne du Rouvray, France) and the *Institut de Développement des Ressources en Informatique Scientifique* (IDRIS-CNRS, Orsay, France).

REFERENCES

1 Cushman J.H. (1997) *The Physics of Fluids in Hierarchical Porous Media: Angstroms to Miles*, Kluwer Academic Publishers, London.

2 Guéguen Y., Palciauskas V. (1994) *Introduction to the physics of rock*, University Press, Princeton.

3 Gregg S.J., Sing K.S.W. (1982) *Adsorption, Surface Area and Porosimetry*, Academic Press, New York.

4 Rouquerol F., Rouquerol J., Sing K.S.W. (1999) *Adsorption by Powders and Porous Solids*, Academic Press, London.

5 Zsigmondy R. (1911) Über die Struktur des Gels der Kieselsäure. Theorie der Entwässerung, *Z. Anorg. Allg. Chem.* **71**, 356.

6 Cohan L.H. (1938) Sorption hysteresis and the vapor pressure of concave surfaces, *J. Am. Chem. Soc.* **60**, 433-435.

7 Coasne B., Grosman A., Ortega C., Simon M. (2002) Adsorption in noninterconnected pores open at one or at both ends: A reconsideration of the origin of the hysteresis phenomenon, *Phys. Rev. Lett.* **88**, 256102.

8 Grosman A., Ortega C. (2005) Nature of capillary condensation and evaporation processes in ordered porous materials, *Langmuir* **21**, 10515-10521.

9 Everett D.H., Whitton W.I. (1952) A general approach to hysteresis, *Trans. Faraday Soc.* **48**, 749.

10 Everett D.H., Smith F.W. (1954) A general approach to hysteresis. Part 2: Development of the domain theory, *Trans. Faraday Soc.* **50**, 187.

11 Everett D.H. (1954) A general approach to hysteresis. Part 3: Formal treatment of the independent domain model of hysteresis, *Trans. Faraday Soc.* **50**, 1077.

12 Mason G. (1982) The effect of pore space connectivity on the hysteresis of capillary condensation in adsorption desorption isotherms, *J. Colloid Interface Sci.* **88**, 36-46.

13 Mason G. (1983) A model of adsorption-desorption hysteresis in which hysteresis is primarily developed by the interconnections in a network of pores, *Proc. R. Soc. Lond. A* **390**, 47-72.

14 Swift M.R., Cheng E., Cole M.W., Banavar J.R. (1993) Phase transitions in a model porous medium, *Phys. Rev. B* **48**, 3124.

15 Kierlik E., Rosinberg M.L., Tarjus G., Viot P. (2001) Equilibrium and out-of-equilibrium (hysteretic) behavior of fluids in disordered porous materials: Theoretical predictions, *Phys. Chem. Chem. Phys.* **3**, 1201-1206.

16 Kierlik E., Monson P.A., Rosinberg M.L. *et al.* (2001) Capillary condensation in disordered porous materials: Hysteresis *versus* equilibrium behavior, *Phys. Rev. Lett.* **87**, 055701.

17 Detcheverry F., Kierlik E., Rosinberg M.L., Tarjus G. (2003) Local mean-field study of capillary condensation in silica aerogels, *Phys. Rev. E* **68**, 061504.

18 Detcheverry F., Kierlik E., Rosinberg M.L., Tarjus G. (2006) Gas adsorption and desorption in silica aerogels: a theoretical study of scattering properties, *Phys. Rev. E* **73**, 041511.

19 Beck J.S., Vartuli J.C., Roth W.J. *et al.* (1992) A new family of mesoporous molecular sieves prepared with liquid cristal templates, *J. Am. Chem. Soc.* **114**, 10834-10843.

20 Kresge C.T., Leonowicz M.E., Roth W.J. *et al.* (1992) *Nature* **359**, 710-712.

21 Uhlir A. (1956) Electrolytic shaping of germanium and silicon, *Bell Syst. Tech. J.* **35**, 333-347.

22 Maddox M.W., Olivier J.P., Gubbins K.E. (1997) Characterization of MCM-41 using molecular simulation: heterogeneity effects, *Langmuir* **13**, 1737-1745.

23 Edler K.J., Reynolds P.A., White J.W. (1998) Small-angle neutron scattering studies on the mesoporous molecular sieve MCM-41, *J. Phys. Chem. B* **102**, 3676-3683.

24 Berenguer-Murcia A., Garcia-Martinez J., Cazorla-Amoros D. *et al.* (2002) in *Studies in Surface Science and Catalysis*, Rodriguez Reinoso F., McEnaney B., Rouquerol J., Unger K. (eds), Elsevier Science, Amsterdam, Vol. 144, pp. 83-90.

25 Fenelonov V.B., Derevyankin A.Y., Kirik S.D. *et al.* (2001) Comparative textural study of highly ordered silicate and aluminosilicate mesoporous mesophase materials having different pore sizes, *Micropor. Mesopor. Mater.* **44-45**, 33-40.

26 Sonwane C.G., Jones C.W., Ludovice P.J. (2005) A model for the structure of MCM-41 incorporating surface roughness, *J. Phys. Chem. B* **109**, 23395-23404.

27 Puibasset J. (2005) Grand potential, Helmholtz free energy and entropy calculation in heterogeneous cylindrical pores by the grand canonical Monte Carlo simulation method, *J. Phys. Chem. B* **109**, 480-487.

28 Puibasset J. (2005) Phase coexistence in heterogeneous porous media: A new extension to Gibbs Ensemble monte carlo simulation method, *J. Chem. Phys.* **122**, 134710.

29 Puibasset J. (2005) Capillary condensation in a geometrically and a chemically heterogeneous pore: a molecular simulation study, *J. Phys. Chem. B* **109**, 4700-4706.

30 Puibasset J. (2005) Thermodynamic characterization of fluids confined in heterogeneous pores by Monte Carlo simulations in the grand canonical and the isobaric-isothermal ensembles, *J. Phys. Chem. B* **109**, 8185-8194.

31 Nicholson D., Parsonage N.G. (1982) *Computer Simulation and the Statistical Mechanics of Adsorption*, Academic Press, London.

32 Allen M.P., Tildesley D.J. (1987) *Computer Simulation of Liquids*, Clarendon Press, Oxford.

33 Brown A.J. (1963) *PhD Thesis*, University of Bristol.

34 Gelb L.D., Gubbins K.E., Radhakrishnan R., Sliwinska-Bartkowiak M. (1999) Phase separation in confined systems, *Rep. Prog. Phys.* **62**, 1573-1659.

35 Sarkisov L., Monson P.A. (2001) Modeling of adsorption and desorption in pores of simple geometry using molecular dynamics, *Langmuir* **17**, 7600-7604.

36 Page K.S., Monson P.A. (1996) Monte Carlo calculations of phase diagrams for a fluid confined in a disordered porous material, *Phys. Rev. E* **54**, 6557-6564.

37 Puibasset J., Pellenq R.J.-M. (2004) A grand canonical Monte Carlo simulation study of water adsorption on vycor-like hydrophilic mesoporous silica at different temperatures, *J. Phys. Condens. Matter* **16**, S5329-S5343.

38 Puibasset J., Pellenq R.J.-M. (2004) A comparison of water adsorption on ordered and disordered silica substrates, *Phys. Chem. Chem. Phys.* **6**, 1933-1937.

39 Puibasset J. (2006) Influence of surface chemical heterogeneities on adsorption/desorption hysteresis and coexistence diagram of metastable states within cylindrical pores, *J. Chem. Phys.* **125**, 074707.

40 Detcheverry F., Rosinberg M.L., Tarjus G. (2005) Metastable states and $T = 0$ hysteresis in the random-field Ising model on random graphs, *Eur. Phys. J. B* **44**, 327-343.

41 Pérez-Reche F.J., Rosinberg M.L., Tarjus G. (2008) Numerical approach to metastable states in the zero-temperature random-field Ising model, *Phys. Rev. B* **77**, 064422.

42 Rosinberg M.L., Tarjus G., Pérez-Reche F.J. (2009) The $T = 0$ random-field Ising model on a Bethe lattice with large coordination number: Hysteresis and metastable states, *J. Stat. Mech.* P03003.

43 Puibasset J. (2011) Numerical characterization of the density of metastable states within the hysteresis loop in disordered systems, *J. Phys. Condens. Matter* **23**, 035106.

Final manuscript received in July 2012
Published online in February 2013